

# Cherenkov radiation



In 1934, P.A. Cherenkov observe new type of luminescence irradiating gamma rays into uranyl salt.



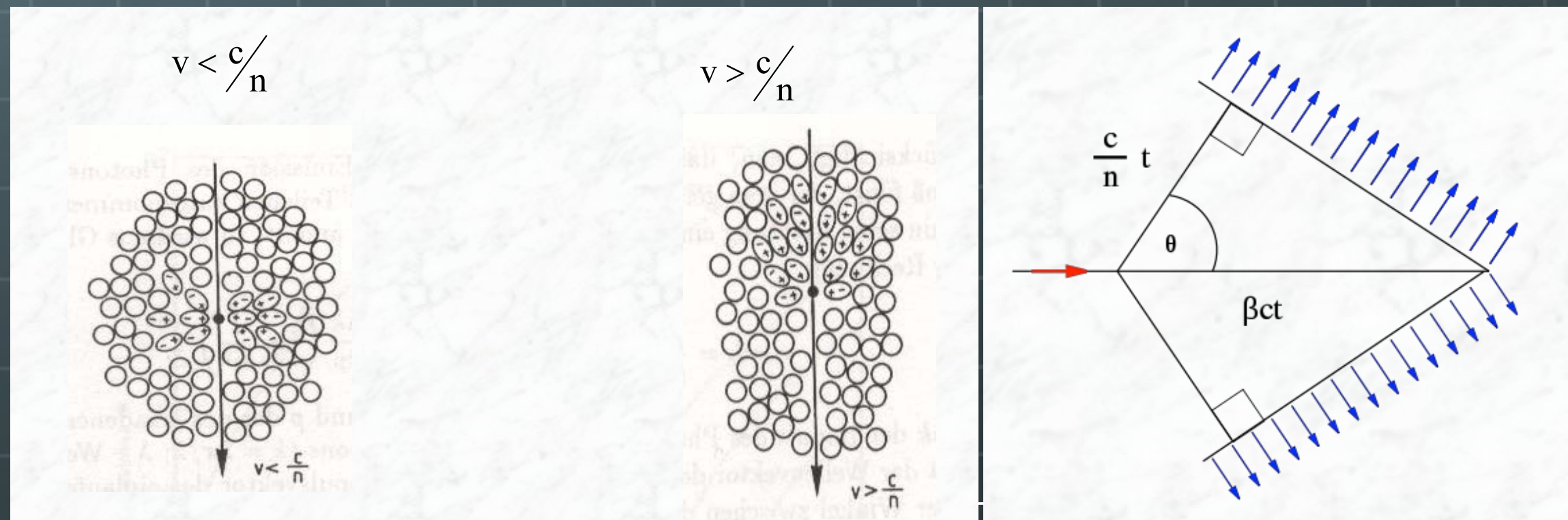
Originated by charged particle



Not to be radiative origin



Observed at a certain angle along particle direction



# Refractive indices, Cherenkov threshold values

Material	$n - 1$	$\beta$ -Schwelle	$\gamma$ -Schwelle
festes Natrium	3.22	0.24	1.029
Bleisulfit	2.91	0.26	1.034
Diamant	1.42	0.41	1.10
Zinksulfid ( $ZnS(Ag)$ )	1.37	0.42	1.10
Silberchlorid	1.07	0.48	1.14
Flintglas (SFS1)	0.92	0.52	1.17
Bleifluorid	0.80	0.55	1.20
Clerici-Lösung	0.69	0.59	1.24
Bleiglas	0.67	0.60	1.25
Thalliumformiat-Lösung	0.59	0.63	1.29
Szintillator	0.58	0.63	1.29
Plexiglas	0.48	0.66	1.33
Borsilikatglas	0.47	0.68	1.36
Wasser	0.33	0.75	1.52
Aerogel	0.025 - 0.075	0.93 - 0.976	4.5 - 2.7
Pentan (STP)	$1.7 \cdot 10^{-3}$	0.9983	17.2
$CO_2$ (STP)	$4.3 \cdot 10^{-4}$	0.9996	34.1
Luft (STP)	$2.93 \cdot 10^{-4}$	0.9997	41.2
$H_2$ (STP)	$1.4 \cdot 10^{-4}$	0.99986	59.8
$He$ (STP)	$3.3 \cdot 10^{-5}$	0.99997	123

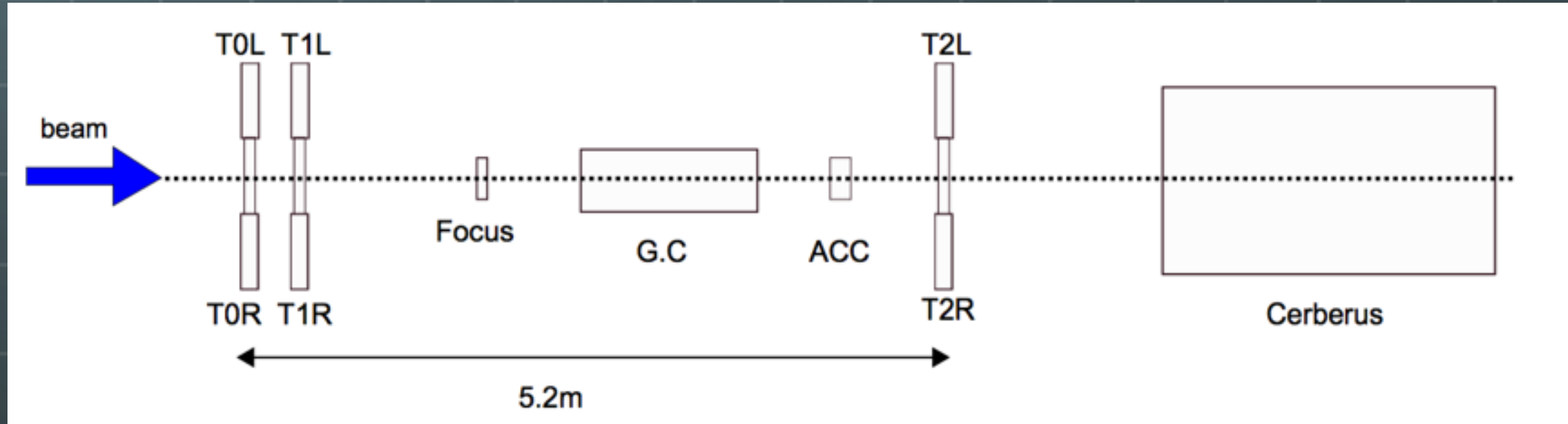
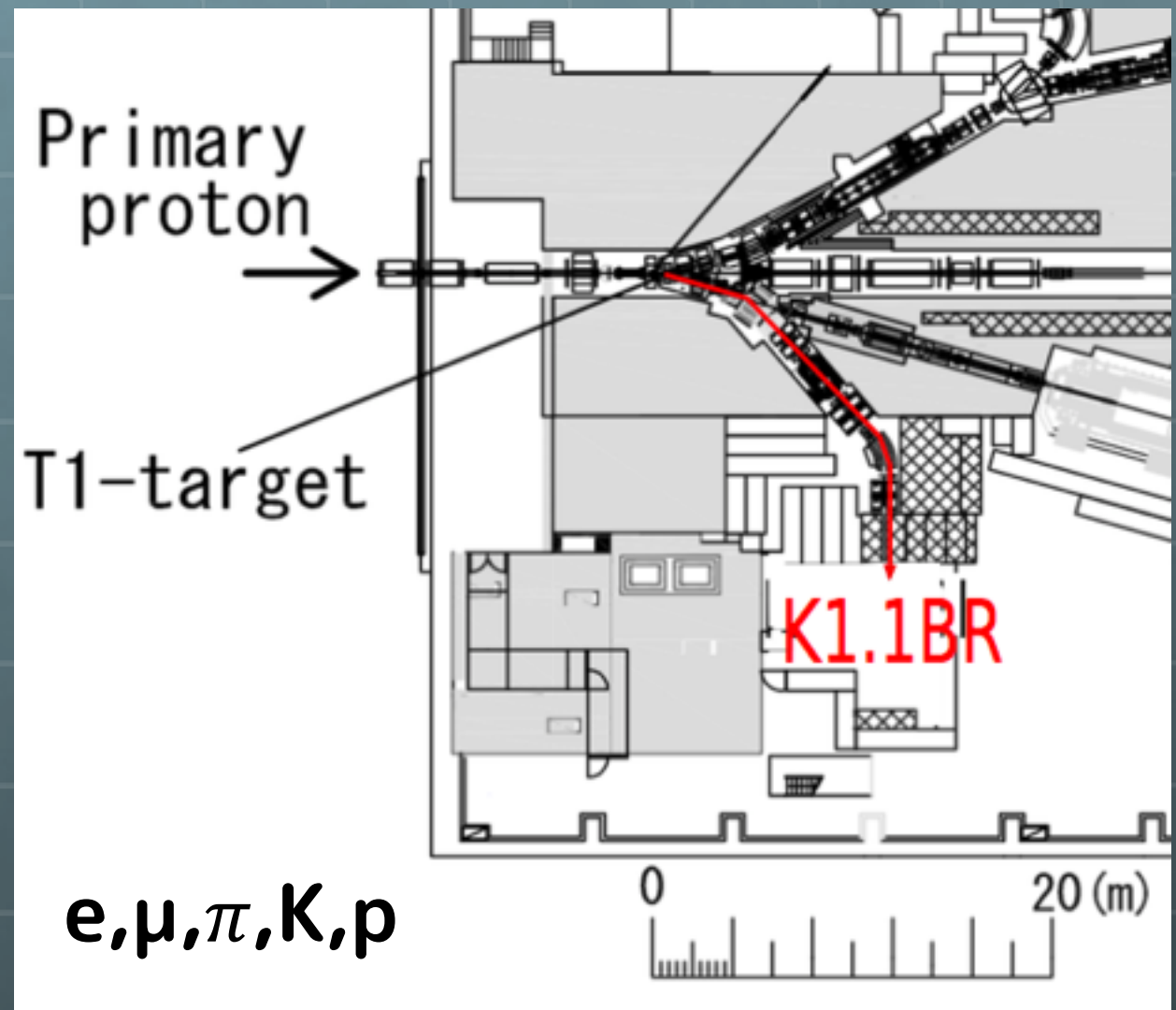
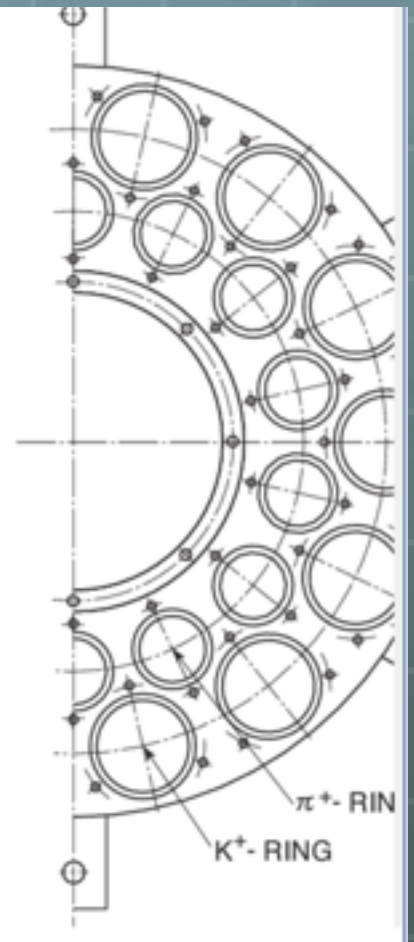
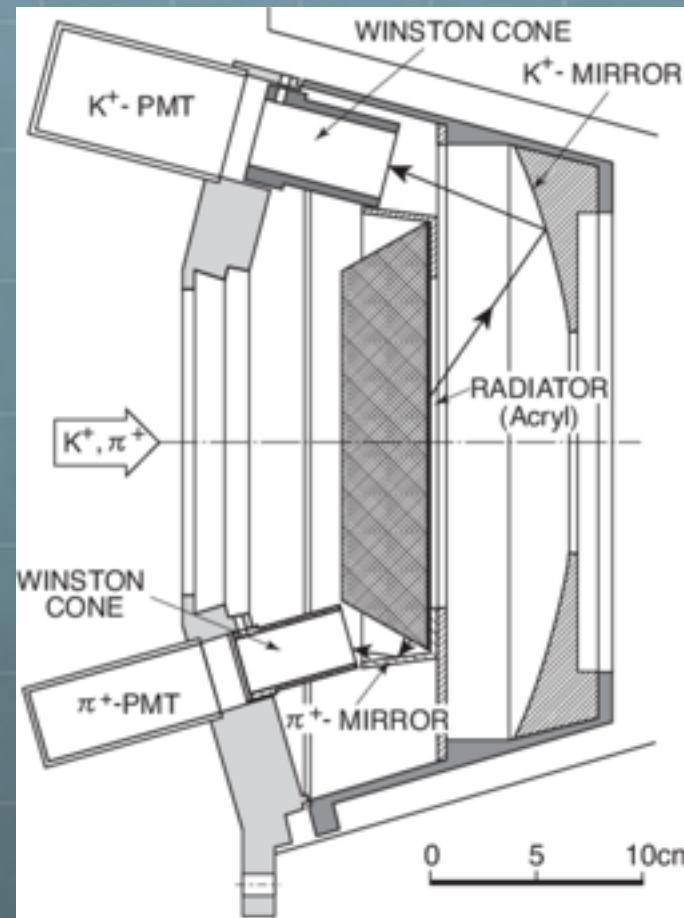
problematic: region between liquids and gases

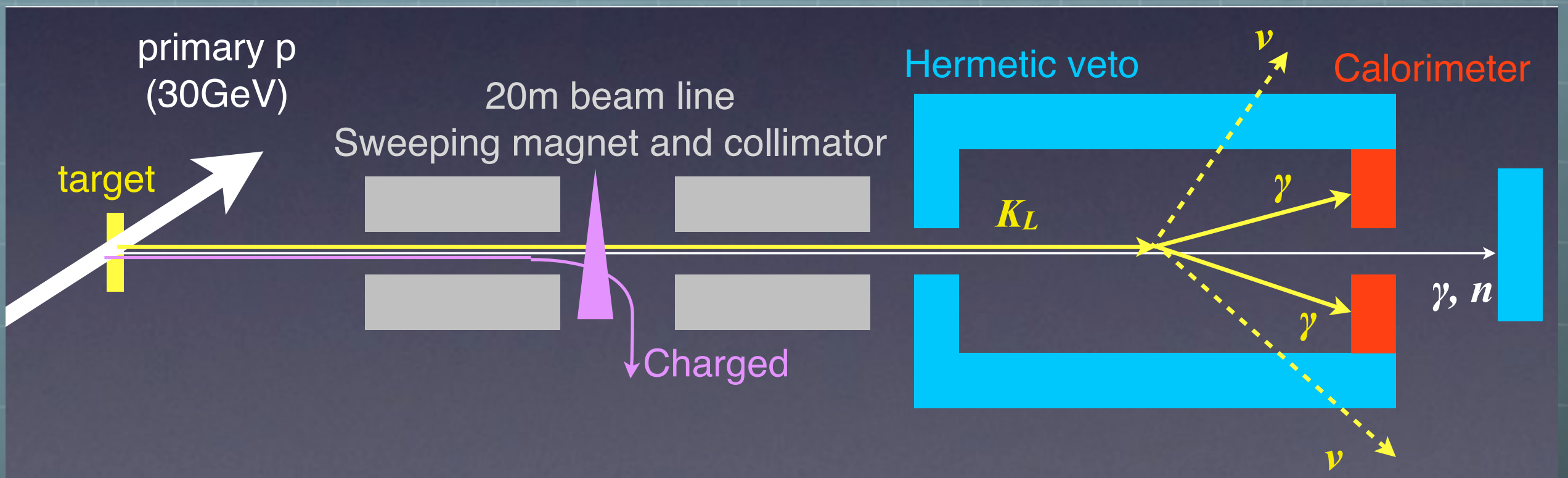
Aerogel: mixture of  $m(SiO_2) + 2m(H_2O)$

light structure with inclusions of air, bubbles with diameter  $< \lambda_{Licht}$

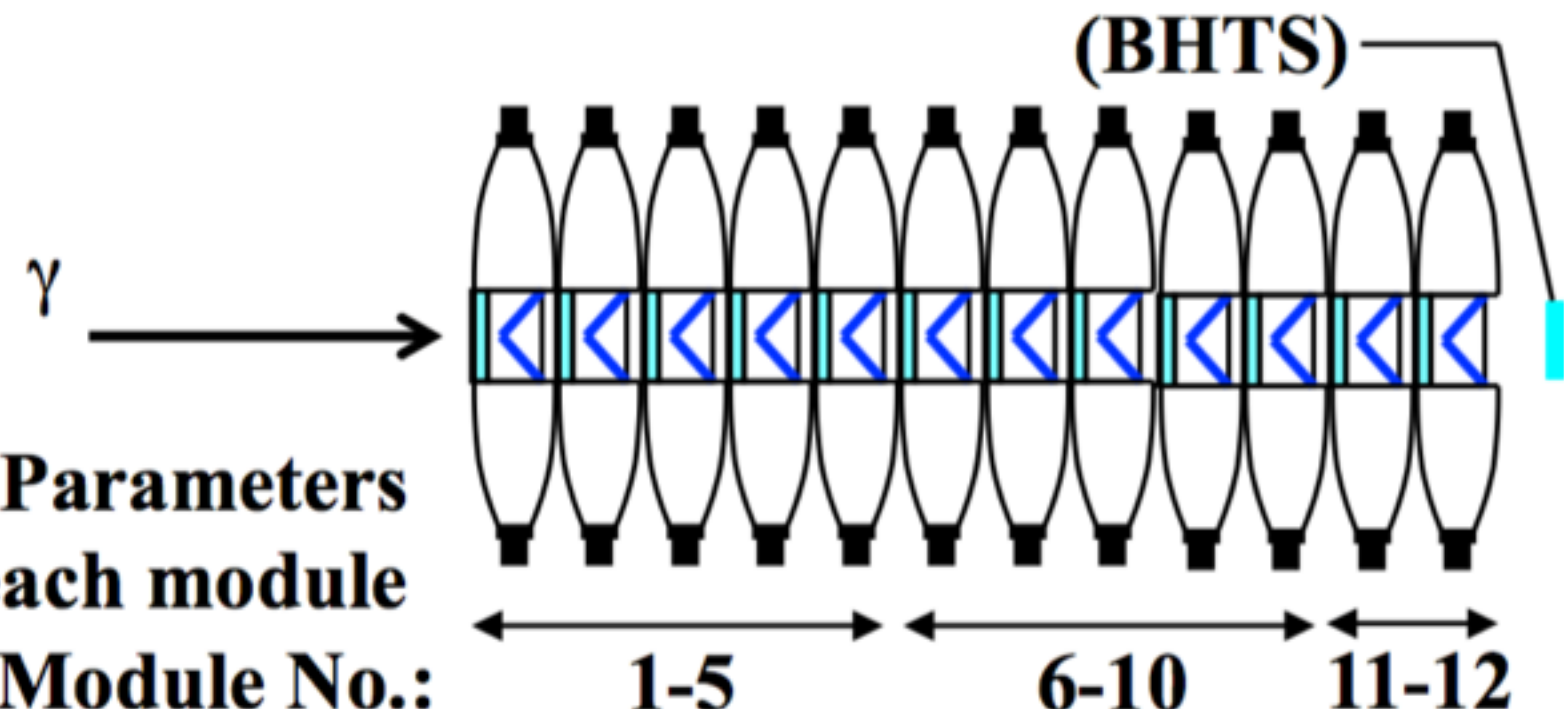
→  $n$ : average from  $n_{air}$ ,  $n_{SiO_2}$ ,  $n_{H_2O}$

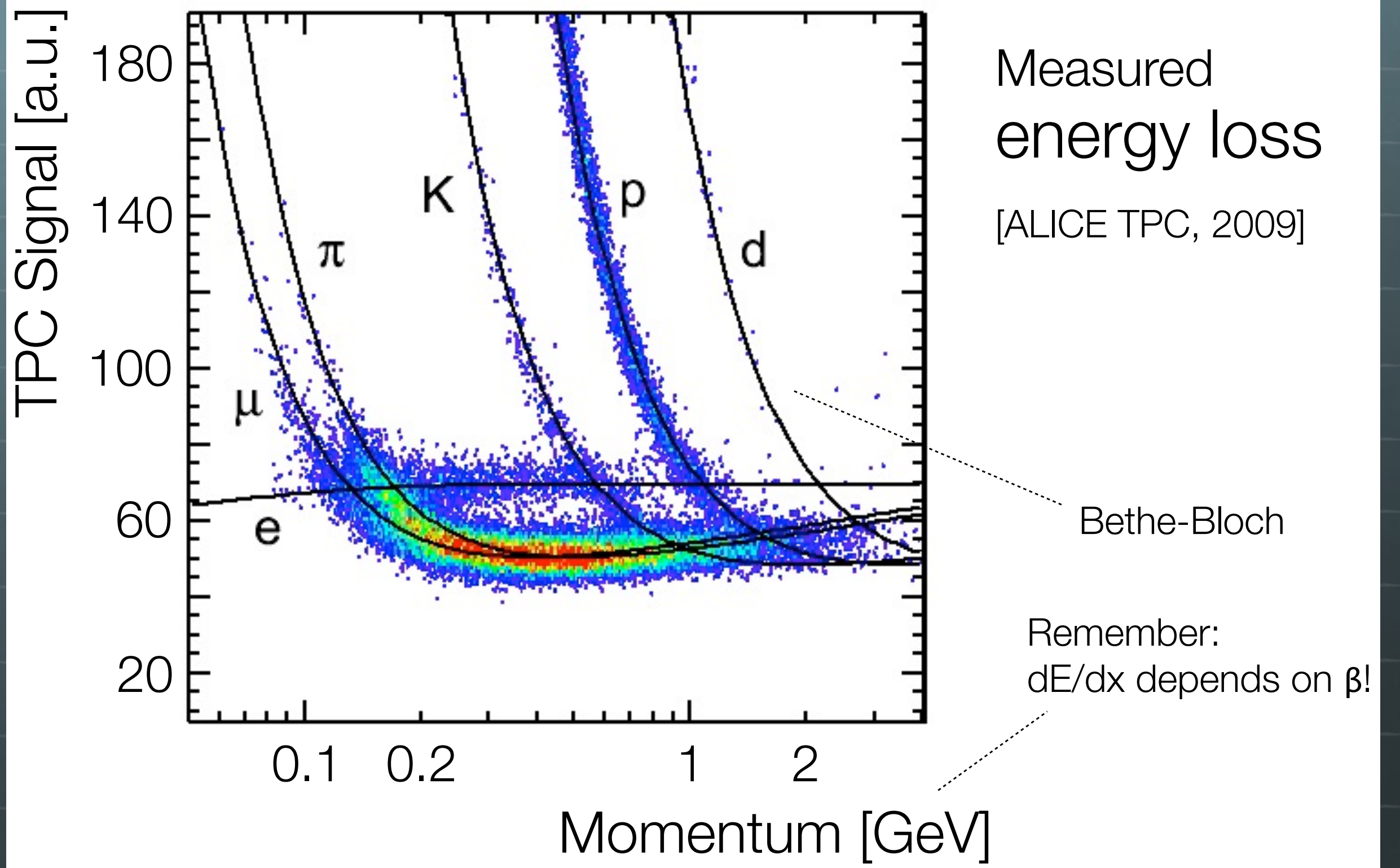
Tabelle 6.2: Cherenkov-Radiatoren [94, 32, 313]. Der Brechungsindex für Gase bezieht sich auf  $0^\circ C$  und  $1\text{ atm}$  (STP). Festes Natrium ist für Wellenlängen unterhalb von  $2000\text{ \AA}$  transparent [373, 209].





## Trigger scintillator for calibration





# Transition radiation (TRD)

Charged particle passes through materials with different dielectric properties

- particle forms dipole with the mirror charge
- dipole changes with time
- radiation

- radiated energy  $W$  proportional to the energy of particle!

$$W = \frac{1}{3} \alpha \hbar \omega_p \gamma$$

- with  $\omega_p$  Plasma frequency

$$\omega_p = \sqrt{\frac{N_e e^2}{\epsilon_0 m_e}} \quad \hbar \omega_p = 20 \text{ eV}$$

- only important for highly relativistic particles

- energy: keV (x-rays)

- $\theta \propto 1/\gamma$  : emission in very forward direction

- probability for photon emission very small → many transitions (foils with gaps)

- # photons  $\langle N \rangle \sim W / h\nu \sim O(\alpha) = 1/137$   $\alpha$  fine structure constant

- energy loss due to TRD negligible for single transition

- important for particle ID at high energies, other effects used for PID  $\propto \beta$  ( $\beta \approx 1$ )

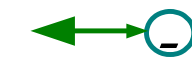
Review article: B. Dolgoshein; NIM A 326 (1993) 434

Air (Vacuum)



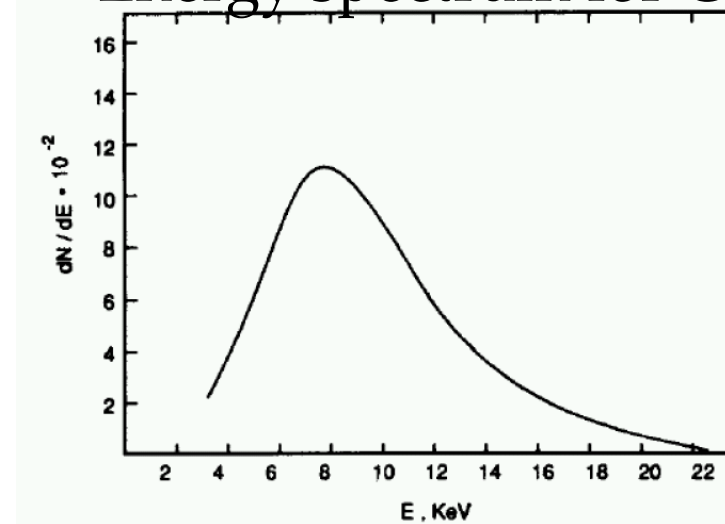
charged part.

Dielectric medium



mirror charge

Energy spectrum for CH<sub>2</sub> foil

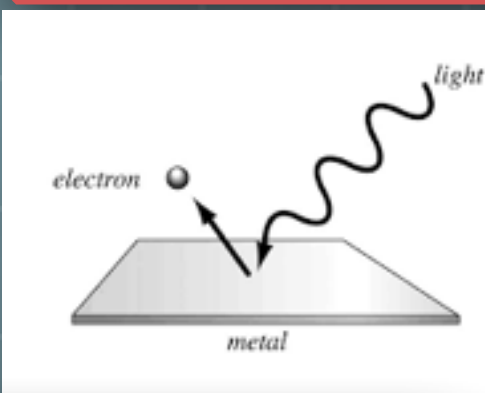


keV!

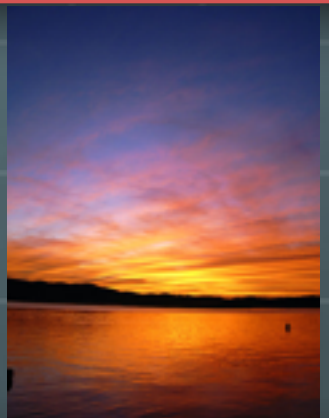
# Interaction of photons

# Interaction of photons

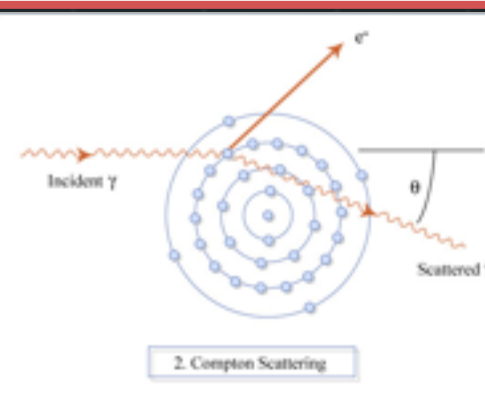
Photoelectric effect



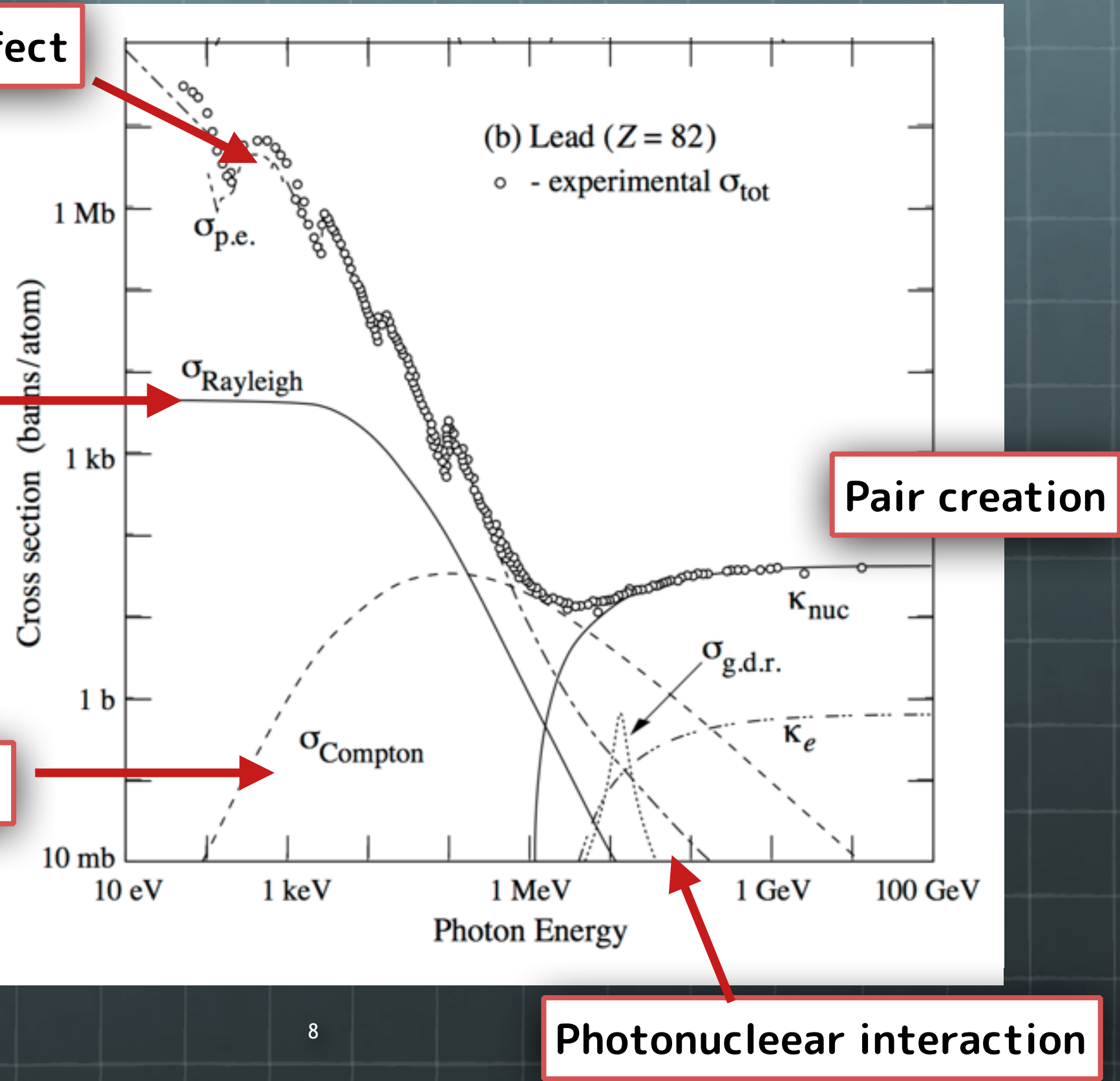
Rayleigh scattering



Compton scattering

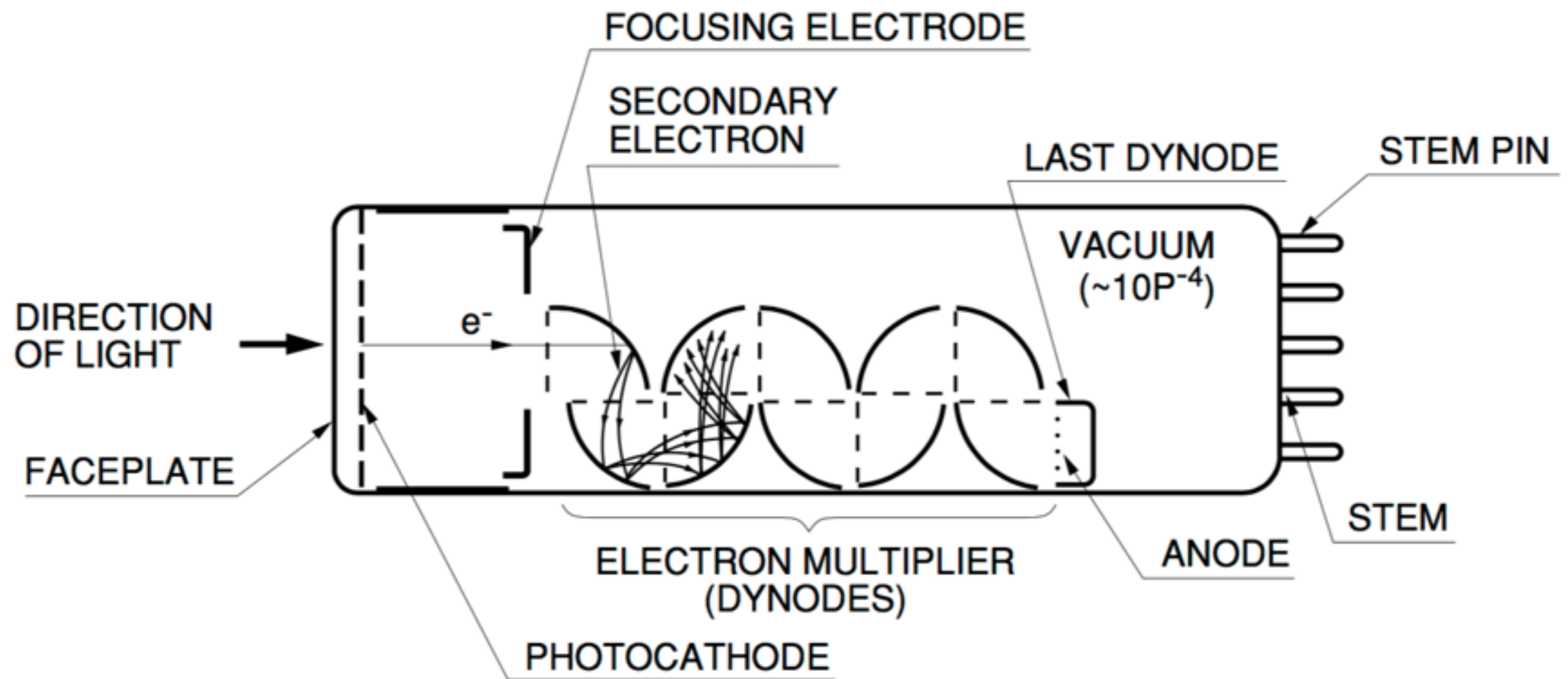


(b) Lead ( $Z = 82$ )  
○ - experimental  $\sigma_{\text{tot}}$



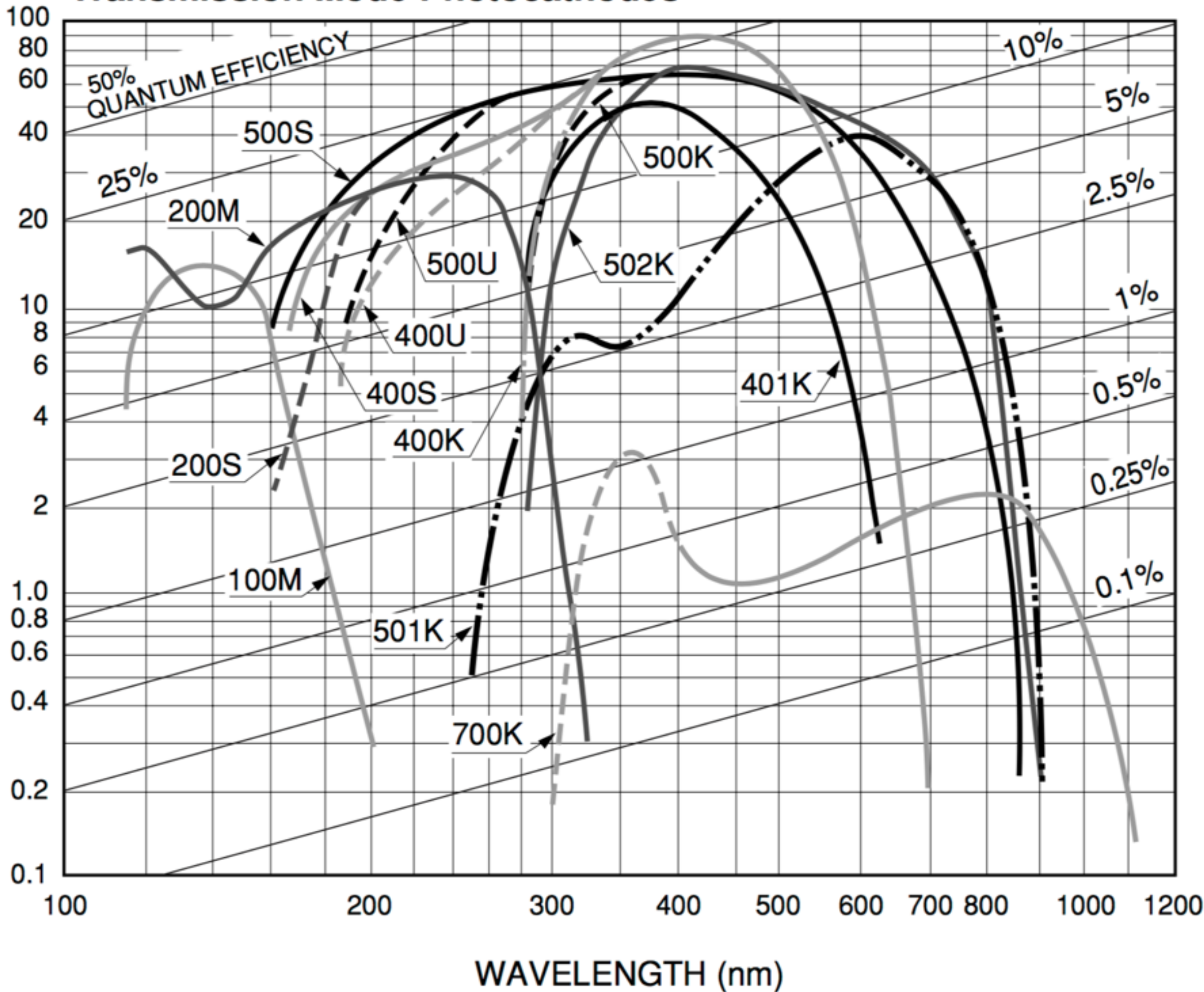
Photonucleolar interaction

# PMT



# Transmission Mode Photocathodes

PHOTOCATHODE RADIANT SENSITIVITY (mA/W)



## Transmission mode photocathodes

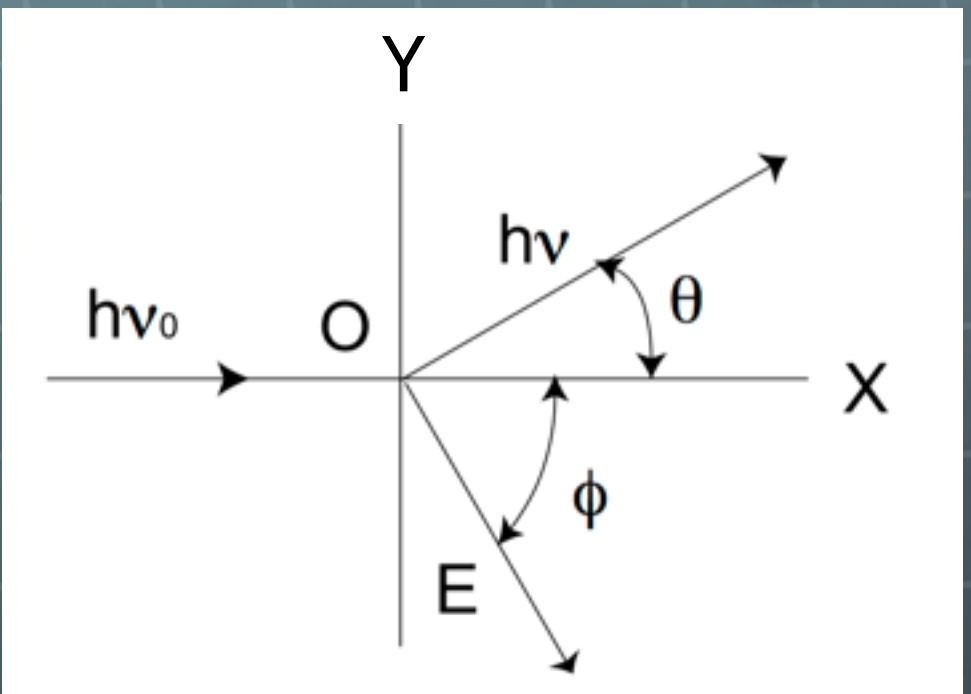
Curve Code (S number)	Photocathode Material	Window Material	Luminous Sensitivity (Typ.) ( $\mu$ A/lm)	Spectral Response				
				Spectral Range (nm)	Peak Wavelength			
					Radiant Sensitivity (mA/W)		(%)	(nm)
100M	Cs-I	MgF <sub>2</sub>	—	115 to 200	14	140	13	130
200S	Cs-Te	Quartz	—	160 to 320	29	240	14	210
200M	Cs-Te	MgF <sub>2</sub>	—	115 to 320	29	240	14	200
400K	Bialkali	Borosilicate	95	300 to 650	88	420	27	390
400U	Bialkali	UV	95	185 to 650	88	420	27	390
400S	Bialkali	Quartz	95	160 to 650	88	420	27	390
401K	High temp. bialkali	Borosilicate	40	300 to 650	51	375	17	375
500K (S-20)	Multialkali	Borosilicate	150	300 to 850	64	420	20	375
500U	Multialkali	UV	150	185 to 850	64	420	25	280
500S	Multialkali	Quartz	150	160 to 850	64	420	25	280
501K (S-25)	Multialkali	Borosilicate	200	300 to 900	40	600	8	580
502K	Multialkali	Borosilicate (prism)	230	300 to 900	69	420	20	390
700K (S-1)	Ag-O-Cs	Borosilicate	20	400 to 1200	2.2	800	0.36	740
—	GaAsP(Cs)	—	—	300 to 720	180	580	40	540
—	GaAs(Cs)	—	—	380 to 890	85	800	14	760
—	InP/InGaAsP(Cs)	—	—	950 to 1400	21	1300	2.0	1000 to 1300
—	InP/InGaAs(Cs)	—	—	950 to 1700	24	1500	2.0	1000 to 1550

# Compton Scattering

$$h\nu = \frac{h\nu_0}{1 + \left(\frac{h\nu_0}{m_e c^2}\right)(1 - \cos \theta)},$$

$$E = h\nu_0 - h\nu = m_e c^2 \frac{2(h\nu_0)^2 \cos^2 \phi}{(h\nu_0 + m_e c^2)^2 - (h\nu_0)^2 \cos^2 \phi},$$

$$\tan \phi = \frac{1}{1 + \left(\frac{h\nu_0}{m_e c^2}\right)} \cot \frac{\theta}{2},$$



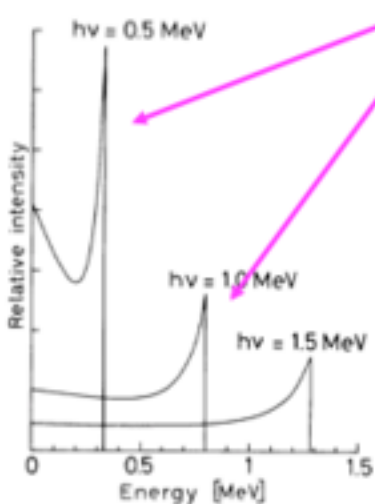
We can also calculate the recoil kinetic energy ( $T$ ) spectrum of the electron:

$$\frac{d\sigma}{dT} = \frac{\pi r_e^2}{m_e c^2 \gamma^2} \left( 2 + \frac{s^2}{\gamma^2 (1-s)^2} + \frac{s}{(1-s)} \left( s - \frac{2}{\gamma} \right) \right) \quad \text{with } s = T / E_{\gamma,in}$$

This cross section is strongly peaked around  $T_{\max}$ :

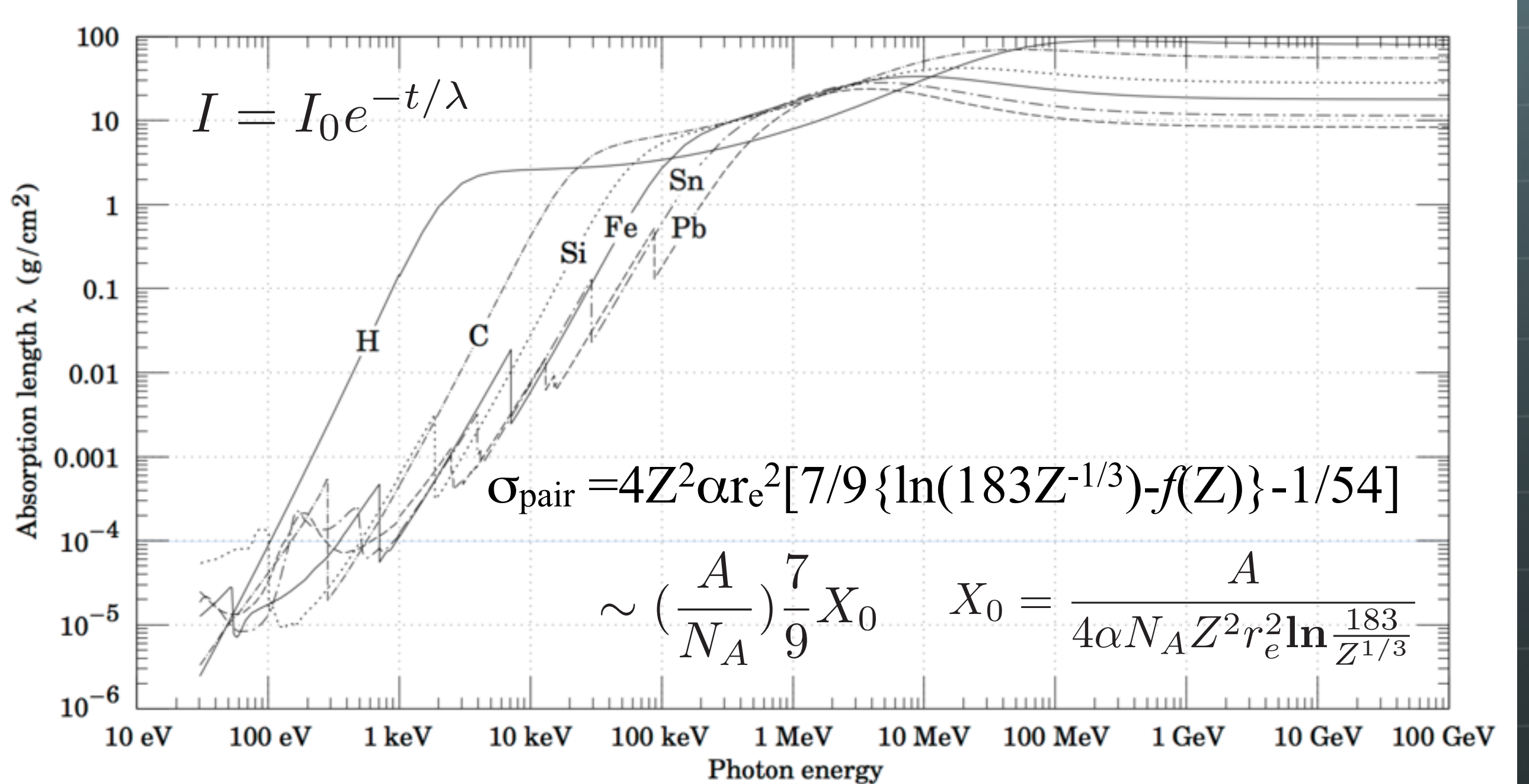
$$T_{\max} = E_{\gamma,in} \frac{2\gamma}{1+2\gamma}$$

$T_{\max}$  is known as the Compton Edge



Kinetic energy distribution of Compton recoil electrons

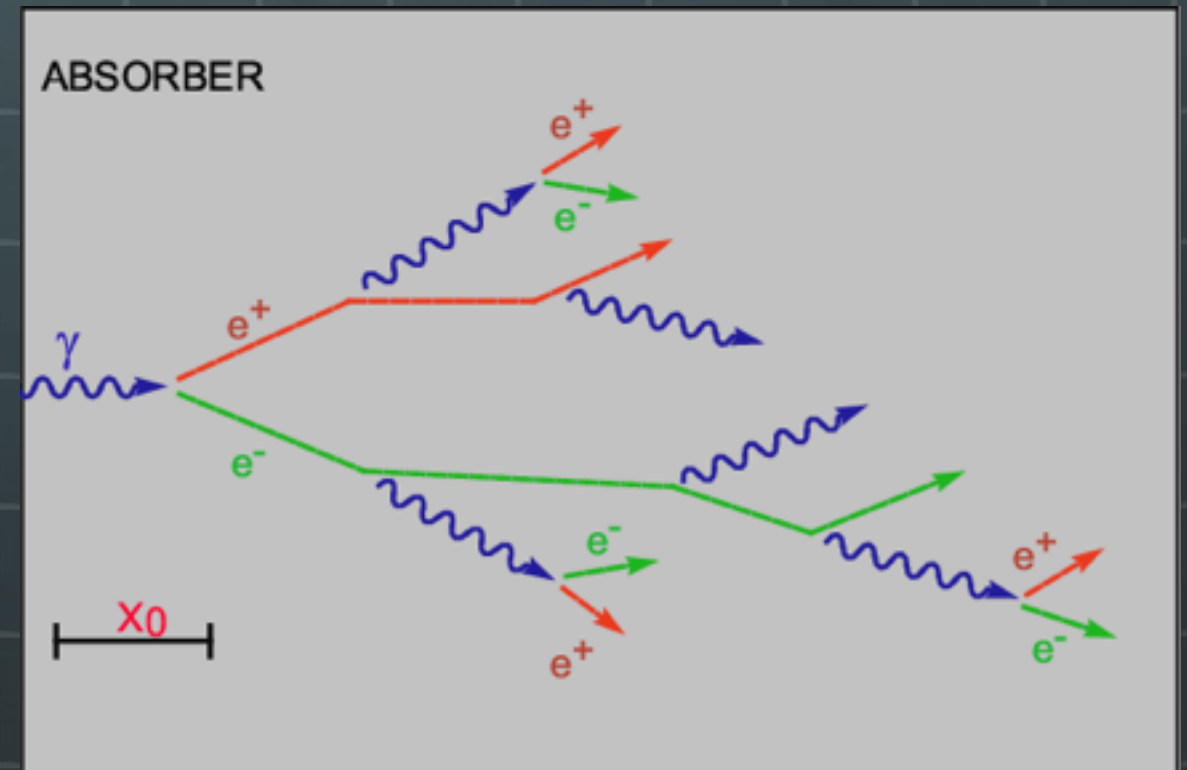
# Pair Production



# Electromagnetic Shower

# Electromagnetic shower

- Electromagnetic calorimeter uses a successive generation of secondaries - EM shower.
- High energy photon occurs pair creation dominantly.
- High energy electron-positron pair loses its energy by bremsstrahlung.



# Radiation Length ( $X_0$ )

- Characteristic amount for energy loss of (high energy) photon and electron
- mean distance over which an electron loses its energy as  $1/e$  by bremsstrahlung
- $7/9$  of the mean free path for pair production by a photon

# Longitudinal shower development



Number of secondaries

$$N = 2^t$$



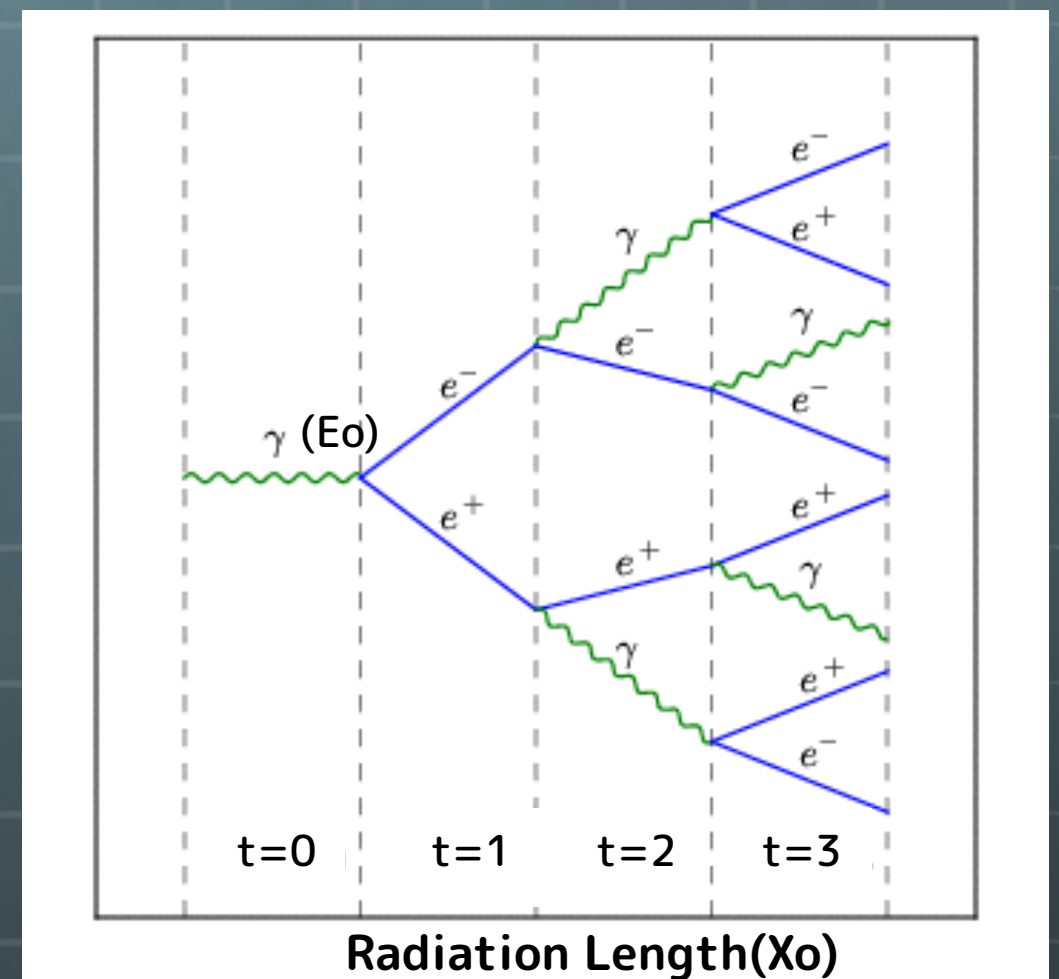
Average Energy

$$E(t) = E_0/2^t$$



Shower development stops at

$$E(t) = E_c$$



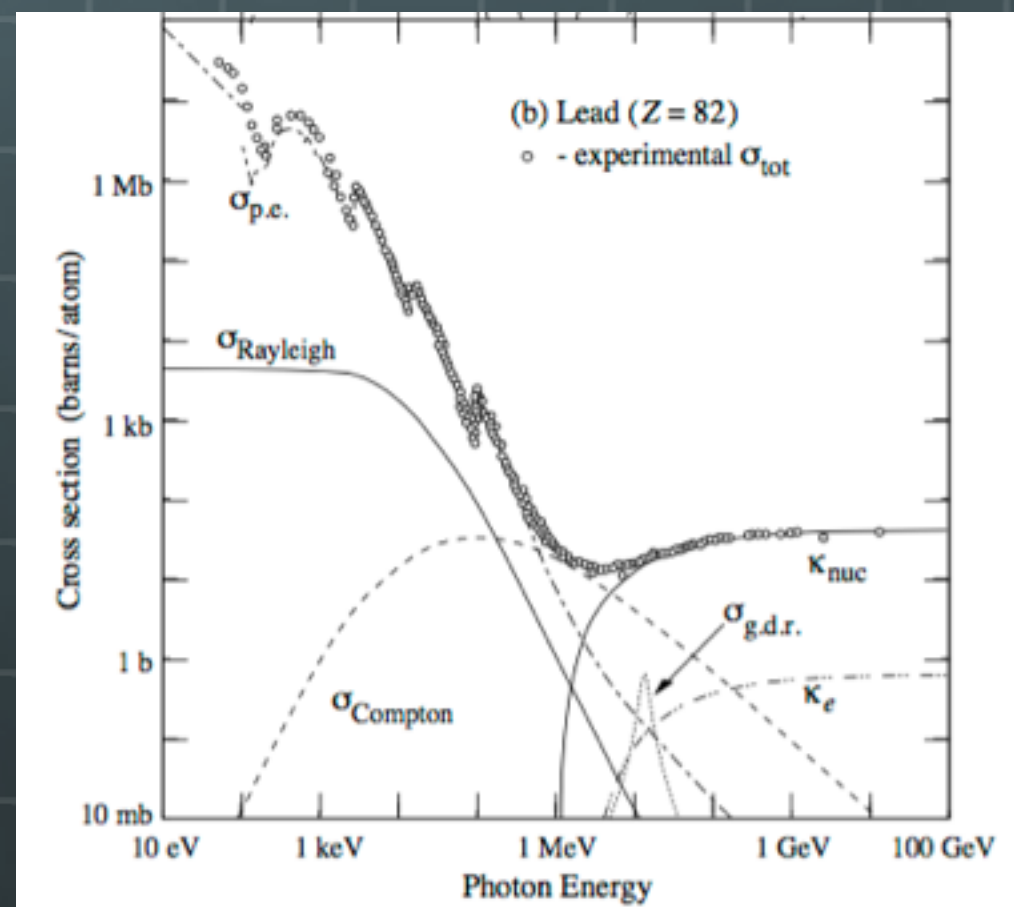
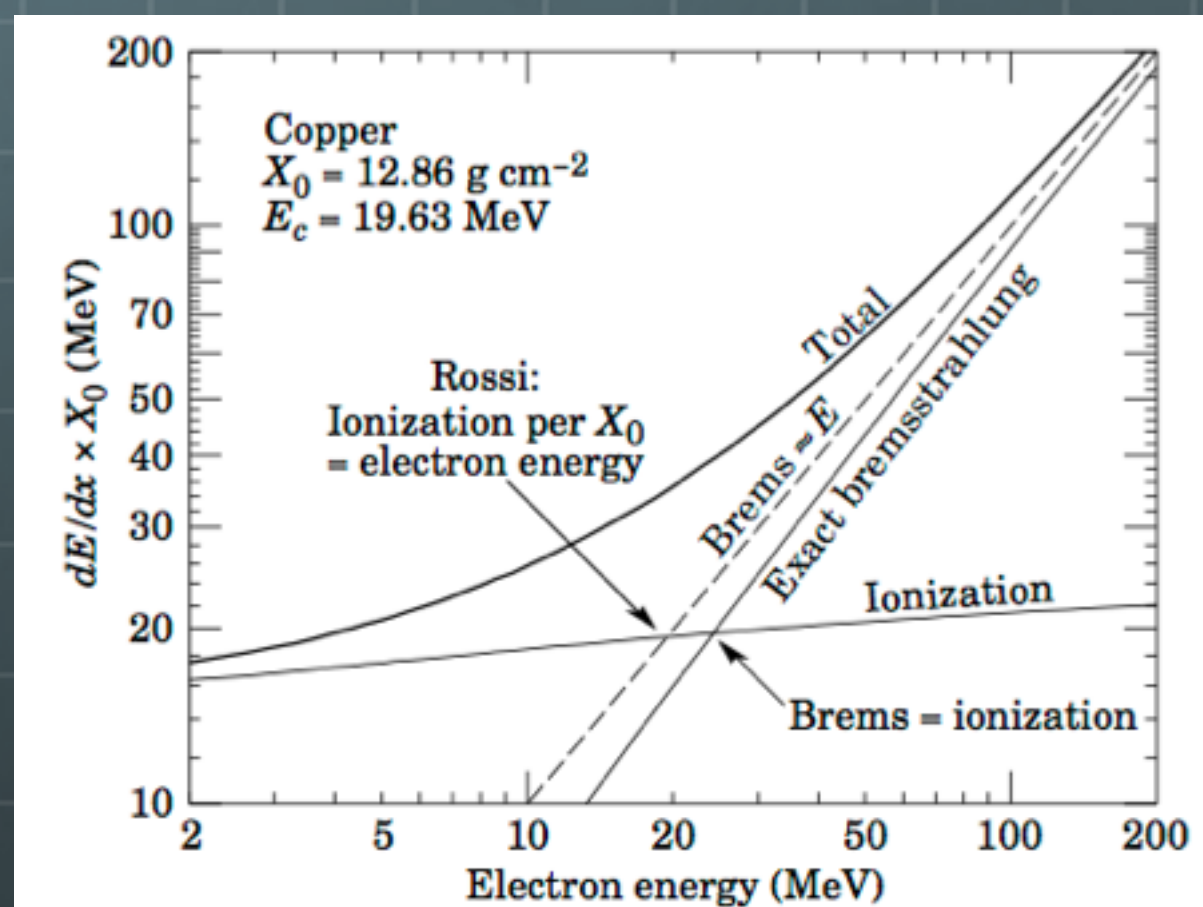
# Critical energy ( $E_c$ )



Energy at which a electron losses its energy as same amount by bremsstrahlung and ionization.



Energy at which the ionization loss per  $X_0$  is equal to the electron energy.



# Longitudinal shower development



Number of secondaries

$$N = 2^t$$



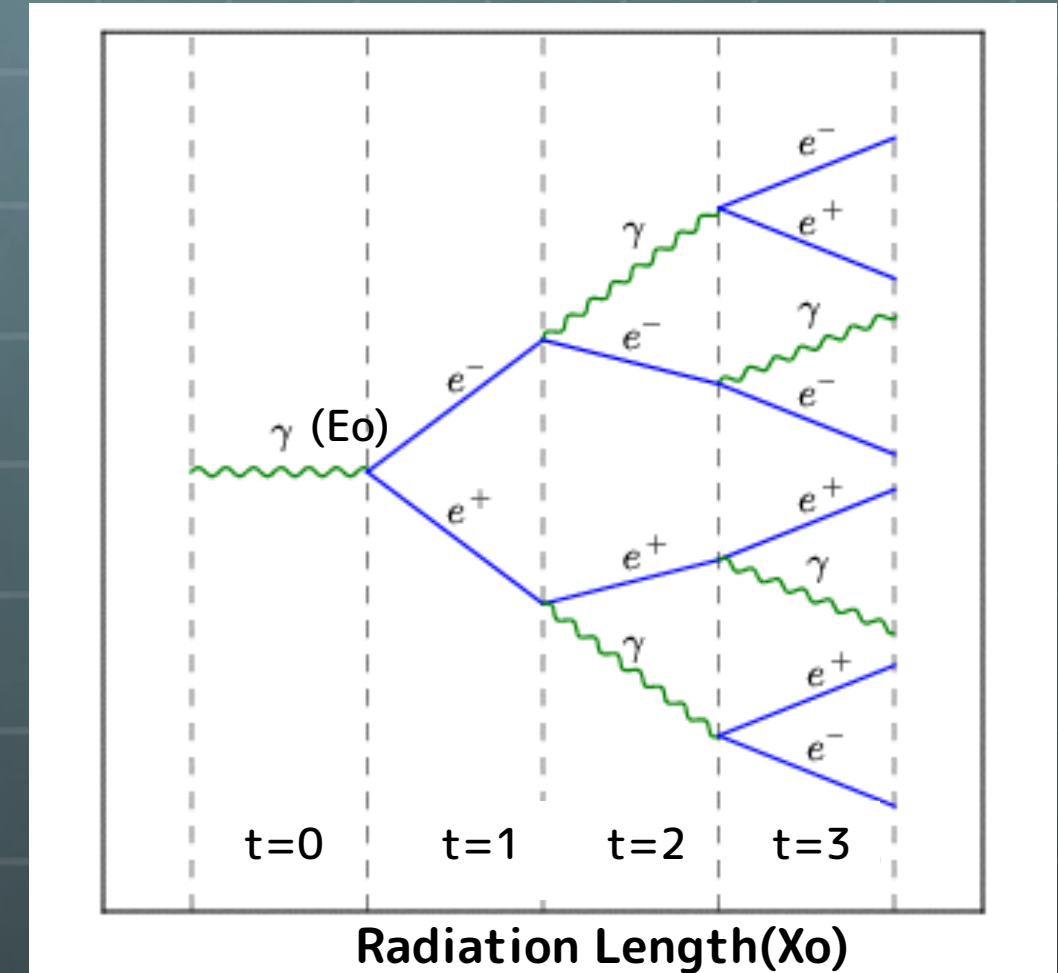
Average Energy

$$E(t) = E_0/2^t$$



Shower development stops at

$$E(t) = E_c$$



Maximum number of shower particles at which their energy is critical energy ;

$$E_c = E_0/2^{t_{max}} \quad t_{max} = \ln\left(\frac{E_0}{E_c}\right)/\ln 2$$

# Energy deposit



Energy deposit  $\propto$  total integrated charged track length

$$\langle T_i(E_0) \rangle = \int_{(i-1)\Delta t}^{i\Delta t} N(E_0, E_{th}, t) dt$$

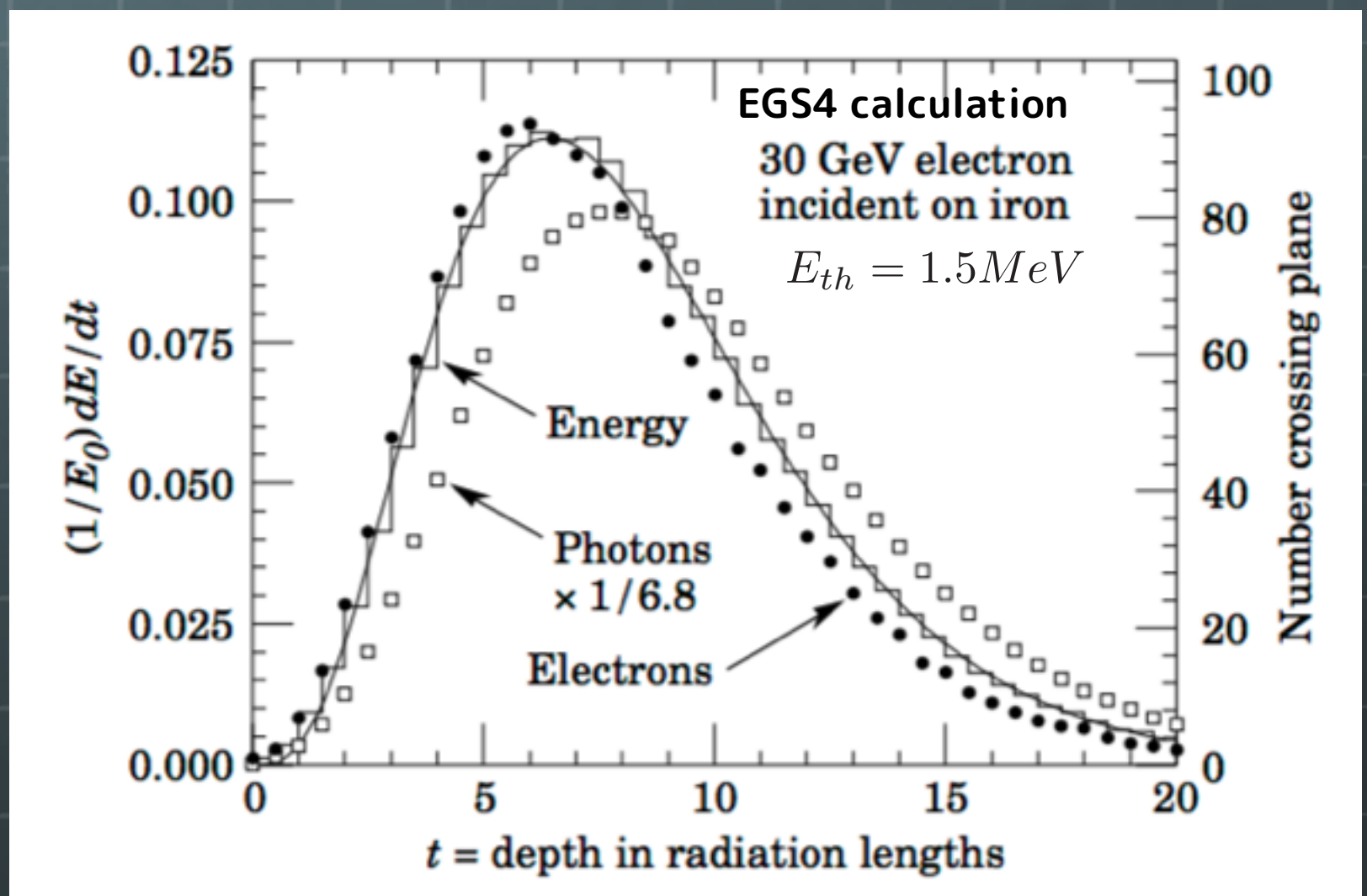
$$\frac{dE}{dx} = E_0 b \frac{(bt)^{(a-1)} e^{-bt}}{\Gamma(a)}$$

$$t_{max}\left(\frac{dE}{dx}\right) = (a - 1)/b$$

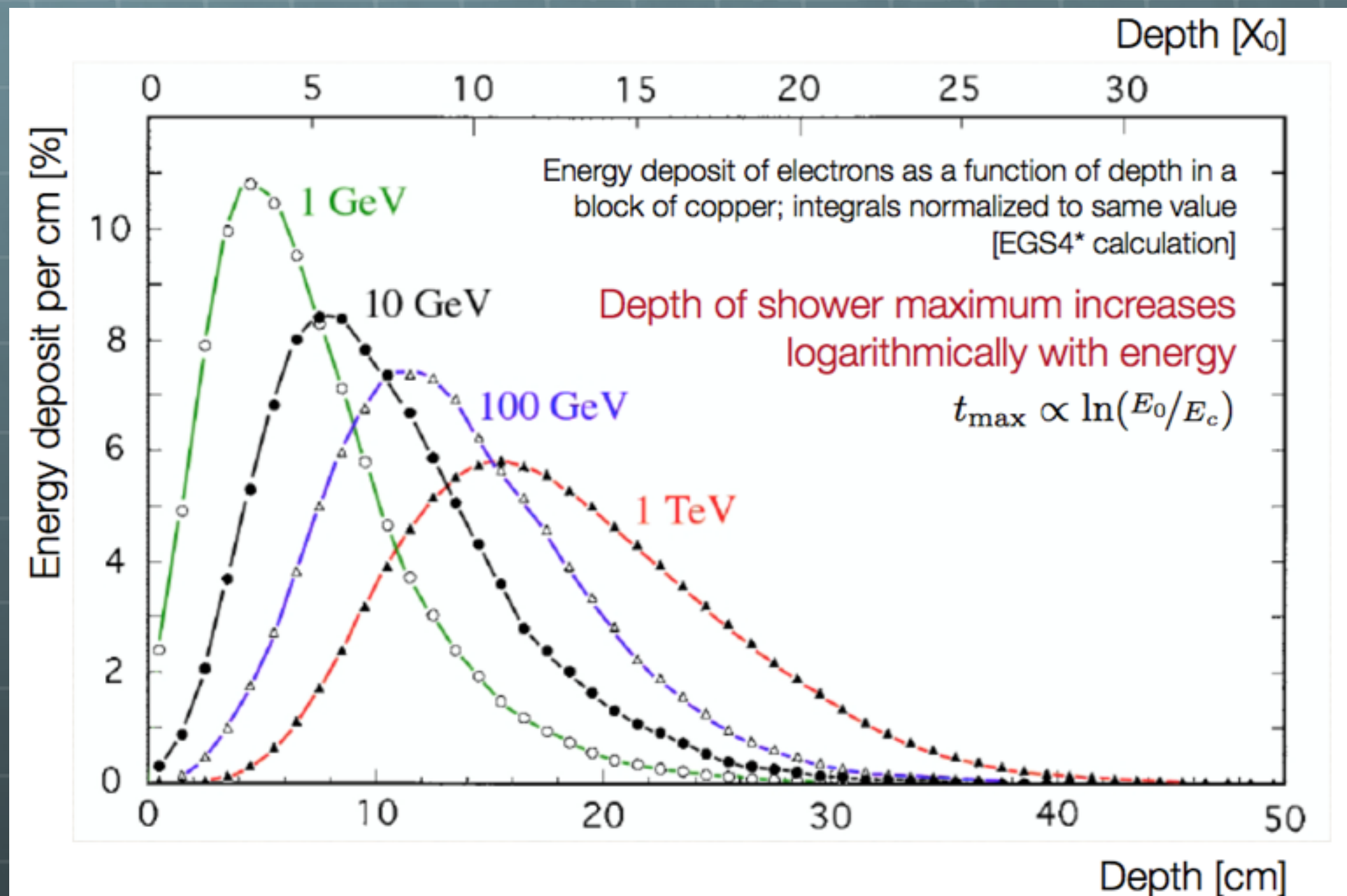
$$= \ln\left(\frac{E_0}{E_c}\right) + C_j$$

$$C_e = -0.5$$

$$C_\gamma = +0.5$$



# Longitudinal shower shape



# Lateral development of EM



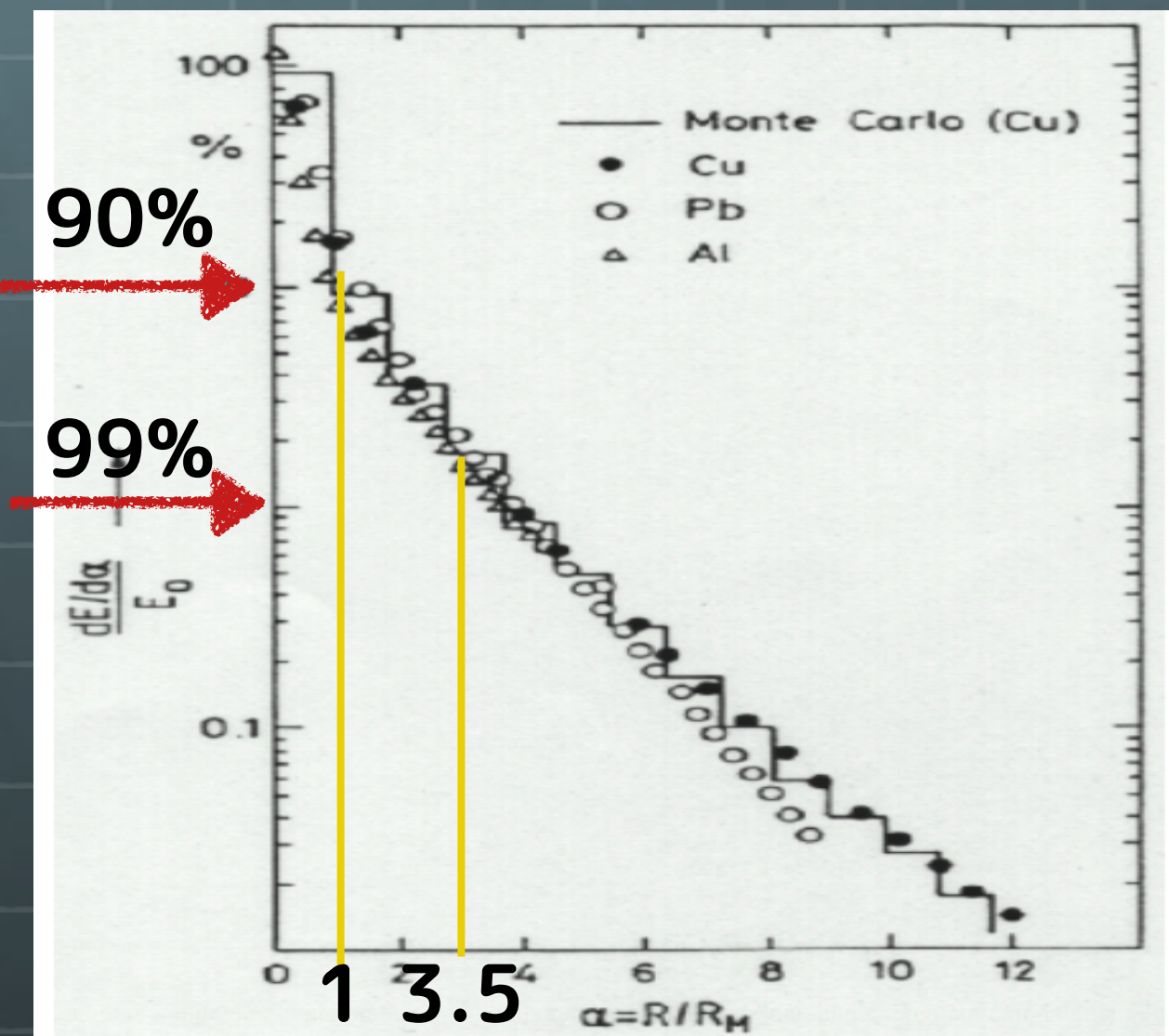
Mainly due to multiple scattering of low energy electron.



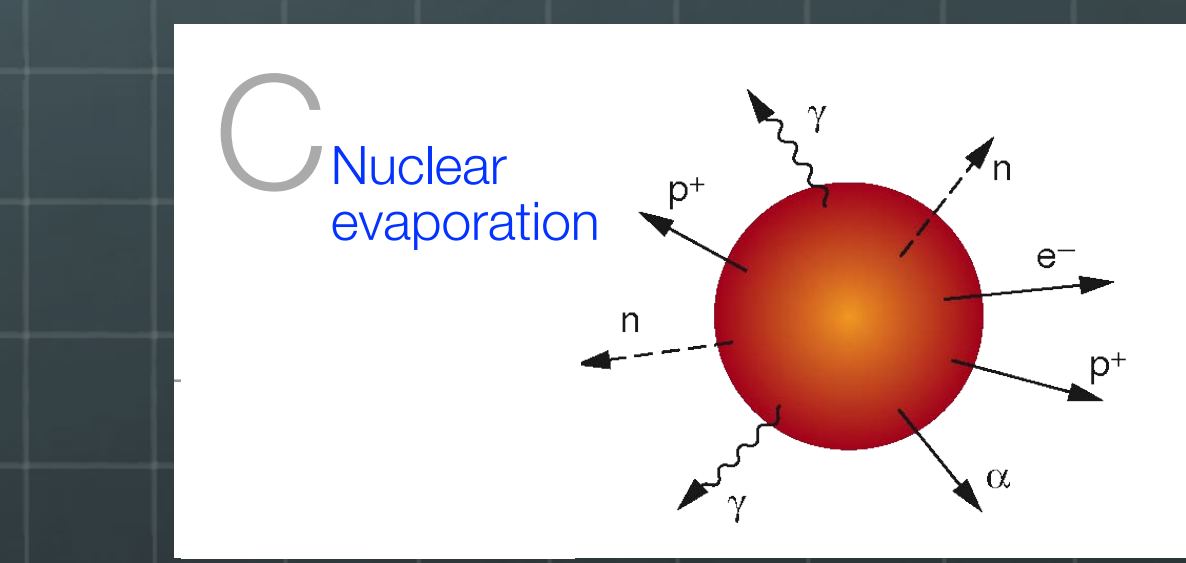
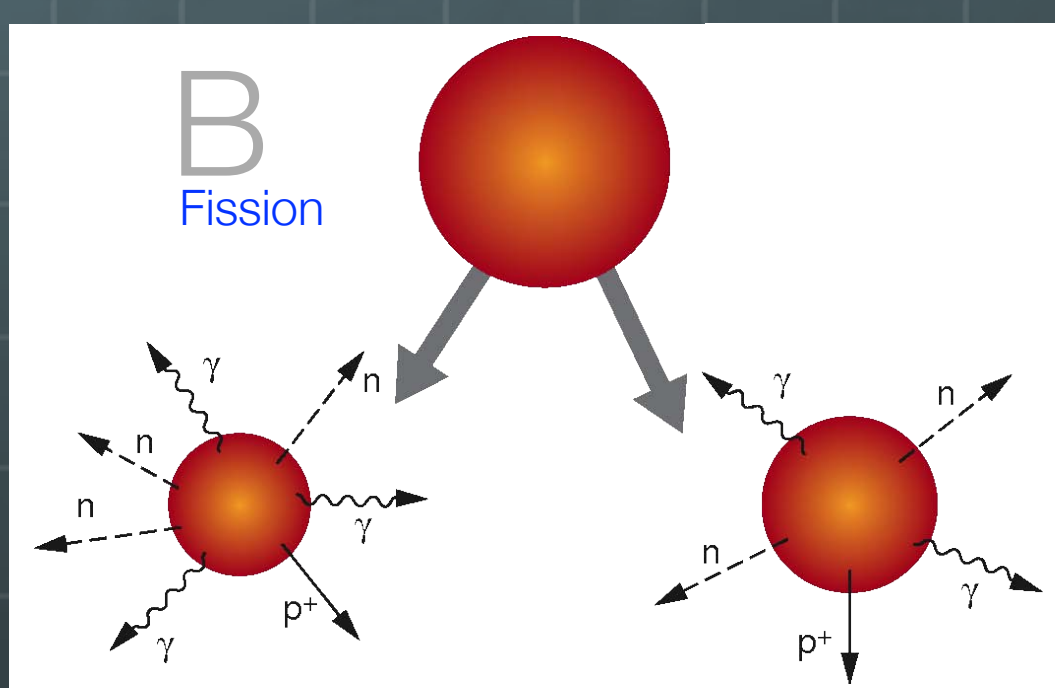
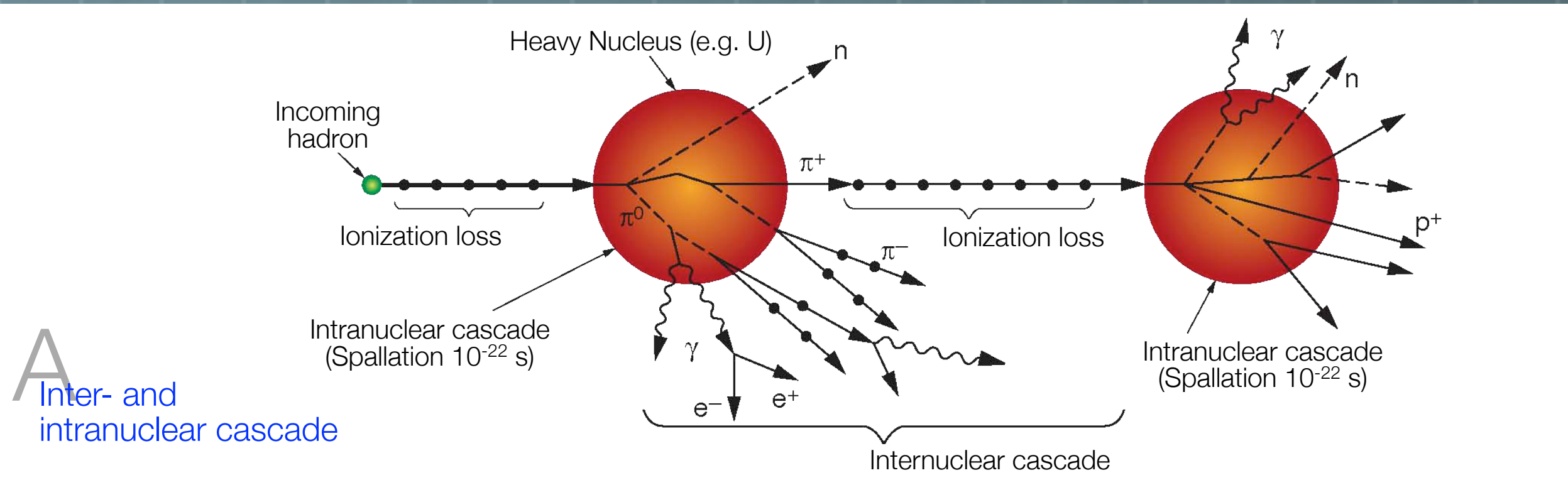
Moirère Radius ( $R_M$ )

$$R_M = \frac{21 \text{ MeV}}{E_c} X_0$$

$$\sim \frac{7A}{Z} [\text{g/cm}^2]$$



# Hadronic Shower



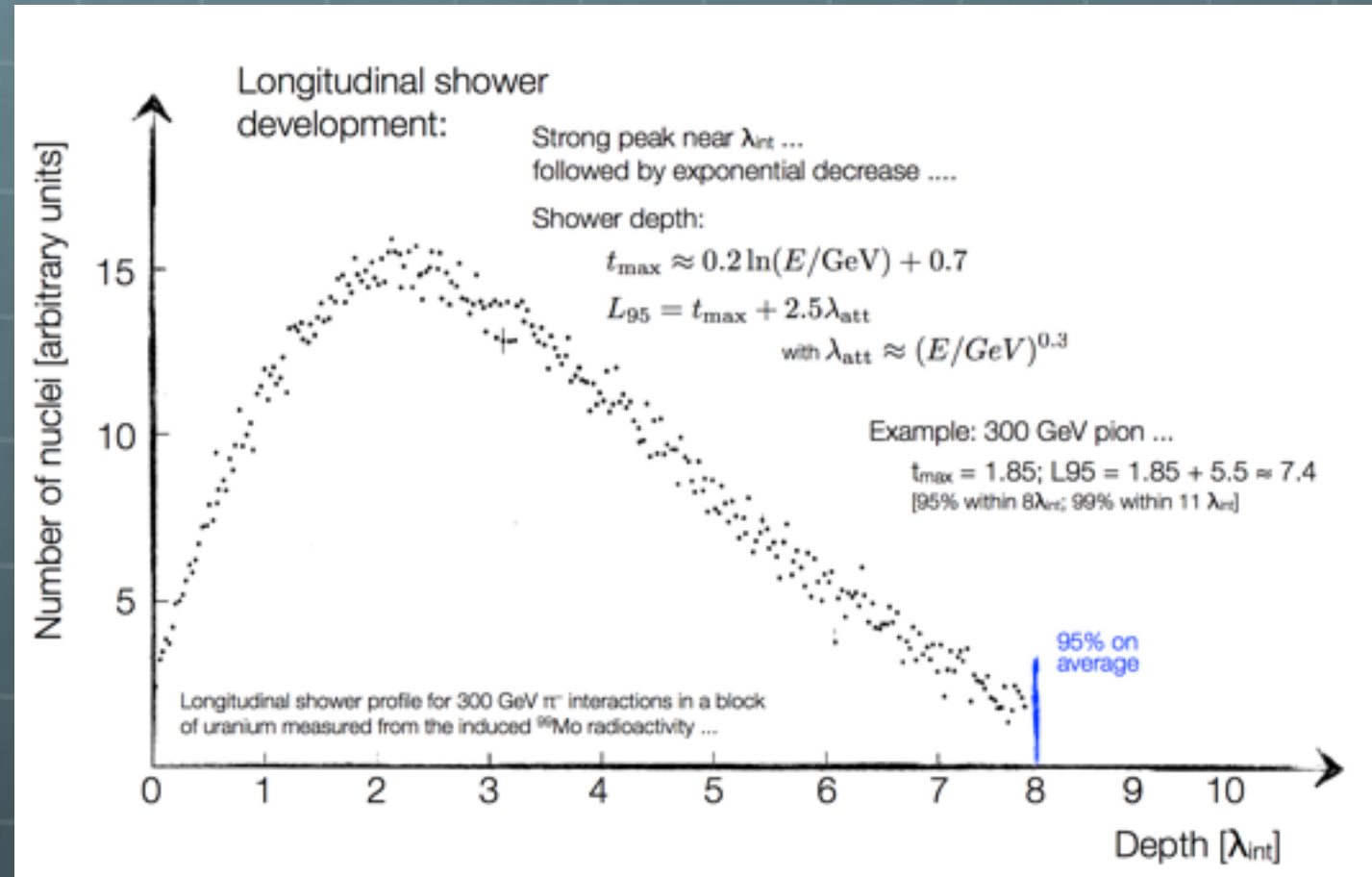
# Hadronic shower

$$\lambda_I \approx 35 \text{ g/cm}^2 \cdot A^{\frac{1}{3}}$$

$$N(x) = N_0 e^{-\frac{x}{\lambda_I}}$$

Typical  
Longitudinal size: 6 ... 9  $\lambda_{\text{int}}$   
[95% containment]

Typical  
Transverse size: one  $\lambda_{\text{int}}$   
[95% containment]



	$\lambda_I$	$X_0$	$R=(\lambda_I/X_0)$		$\lambda_I$	$X_0$	$R=(\lambda_I/X_0)$
Fe	16.78	1.76	9.54	Scin.	78.93	42.62	1.85
Cu	15.32	1.44	10.68	CsI	38.03	1.86	20.44
Pb	17.59	0.56	31.33	PbWO <sub>4</sub>	20.28	0.89	22.77

# Comparison hadronic vs EM showers

